

Effect of the Distribution of Manganese Ions on the Properties of Mn-Doped (Ba,Y)TiO₃ PTCR Ceramics

O. I. V'yunov, L. L. Kovalenko, A. G. Belous, and V. N. Belyakov

*Vernadsky Institute of General and Inorganic Chemistry, National Academy of Sciences of Ukraine,
pr. Akademika Palladina 32/34, Kiev-142, 03680 Ukraine*

e-mail: belous@ionc.kar.net

Received April 3, 2002

Abstract—The electrical properties and microstructure of (Ba,Y)TiO₃ PTCR ceramics were studied. The results indicate that the Mn ions increase the intergranular barrier height and produce a high-resistance layer on the grain surface. The temperature-dependent resistances of the grain bulk, surface layer, and grain boundaries, the temperature coefficient of resistance, and the magnitude of the varistor effect were assessed as a function of Mn content.

INTRODUCTION

(Ba,Y)TiO₃ ceramics exhibit a positive temperature coefficient of resistance (PTCR) at the temperature of the transition from the tetragonal, ferroelectric phase to the cubic, paraelectric phase [1]. A necessary condition for this effect is the formation of potential barriers at grain boundaries. For this reason, in fabricating BaTiO₃-based PTCR ceramics, efforts are focused on producing high-resistivity grain boundaries and semiconducting grains. This can be achieved by introducing small additions of rare-earth ions into the barium sublattice and oxidizing the grain boundaries via air sintering.

Complex impedance and electric modulus measurements over a broad frequency range [2–4] confirm that such materials consist of semiconducting grains, with a higher resistance outer layer and high-resistance grain boundaries. This structure can be represented by an equivalent circuit comprising three parallel RC circuits connected in series.

BaTiO₃-based PTCR materials are characterized by a relatively small ρ_{\max}/ρ_{\min} ratio in the PTCR region and a sizeable varistor effect (a decrease in resistivity in an applied electric field), which is a serious impediment to high-field applications of such materials. It is well known that acceptor doping, in particular with manganese ions, improves the PTCR behavior of BaTiO₃-based materials, changing the grain-boundary resistance [5]. The reason for the significant effect of the Mn dopant on the PTCR behavior of barium titanate is that the redox processes in manganese oxides and partial Ti⁴⁺ \longleftrightarrow Ti³⁺ transitions in PTCR ceramics occur in the same temperature range [6]. However, the distribution of the Mn acceptor in polycrystalline materials has not yet been studied in sufficient detail, in spite of the fact that such information is crucial for understanding and controlling the properties of PTCR ceramics.

The purpose of this work was to investigate the distribution of manganese ions in PTCR ceramics and its effect on the properties of the grain bulk, surface layer, and grain boundaries.

EXPERIMENTAL

The starting reagents used were extrapure-grade BaCO₃, TiO₂, Y₂O₃, MnSO₄, and aqueous ammonia. To reduce grinding-induced contamination, the inner surfaces of the grinding vessels were lined with vacuum-tight rubber. To achieve a uniform dopant distribution, manganese was introduced via precipitation from solution. In electrical measurements, we used samples sintered at 1340–1360°C. The grain size of ceramics was determined on a JEOL JCSA-733 SuperProbe x-ray microanalyzer. Electrical contacts were made by firing aluminum paste.

We studied both the dc and ac electrical properties of the materials, using a Solartron PGSTAT-30 impedance analyzer in the range 100 Hz to 1 MHz and a VM-560 Q-meter in the range 50 kHz to 35 MHz [7]. The samples were cylindrical in shape, 8 ± 0.1 mm in diameter and 2 ± 0.01 mm in thickness. The components of the equivalent circuit were identified using the Frequency Response Analyzer 4.7 program.

RESULTS AND DISCUSSION

The introduction of manganese into BaTiO₃-based PTCR ceramics increases the ρ_{\max}/ρ_{\min} ratio (Fig. 1) and substantially reduces the magnitude of the varistor effect, which can be characterized by the ρ_e/ρ_0 ratio (normalized resistivity), where ρ_e is the resistivity in an applied electric field and ρ_0 is zero-field resistivity (Fig. 2).

The magnitude of the varistor effect is sensitive to a number of factors, including oxidation of grain boundaries [8, 9]. According to earlier results [10], the varistor effect in yttrium-doped PTCR barium titanate ceramics correlates with the average grain size and is weaker in fine-grained ceramics. The introduction of manganese into PTCR barium titanate notably reduces the magnitude of the varistor effect, without significantly changing the grain size of the ceramics (Fig. 3). This suggests that the weakening of the varistor effect is due to the formation of a high-resistance surface layer at grain boundaries.

Data for $(\text{Ba}_{1-x}\text{Y}_x)\text{TiO}_3$ and Mn-doped $(\text{Ba}_{0.996}\text{Y}_{0.004})\text{TiO}_3$ ceramics can be analyzed in the form of the frequency dependences of complex impedance Z^* , complex admittance Y^* , complex dielectric permittivity ϵ^* , and complex electric modulus M^* [2–4, 11, 12]. These quantities are related by

$$M^* = 1/\epsilon^* = i\omega C_0 Z^* = i\omega C_0 Y^*,$$

where $i = \sqrt{-1}$. Initially, the results were obtained in the form of complex impedance plots $Z''(Z')$, which are convenient for identifying the components of the equivalent circuit. In analyzing experimental data, we also used the frequency dependences of Z'' and M'' . For a parallel RC circuit, the frequency dependences of Z'' and M'' have the form [2–4, 11, 12]

$$Z'' = R \frac{\omega RC}{1 + (\omega RC)^2}, \quad (1)$$

$$M'' = \frac{\epsilon_0}{C} \frac{\omega RC}{1 + (\omega RC)^2}, \quad (2)$$

where $\omega = 2\pi f$ (f is frequency, Hz) and ϵ_0 is the permittivity of vacuum (8.854×10^{-14} F/cm).

Equations (1) and (2) indicate that the frequency dependence of Z'' is sensitive to R (in our case, the resistance of grain boundaries), and that of M'' is influenced by the (low) capacitance in the RC circuit (the capacitance of the grain bulk and surface layer) [2–4].

It follows from Eqs. (1) and (2) that

$$\omega_{\max} = \frac{1}{RC}, \quad (3)$$

$$Z''_{\max} = \frac{R}{2}, \quad (4)$$

$$M''_{\max} = \frac{\epsilon_0}{2C}. \quad (5)$$

Equations (3)–(5) show that the frequencies corresponding to Z''_{\max} and M''_{\max} depend on both R and C . It should be emphasized that the frequency dependences

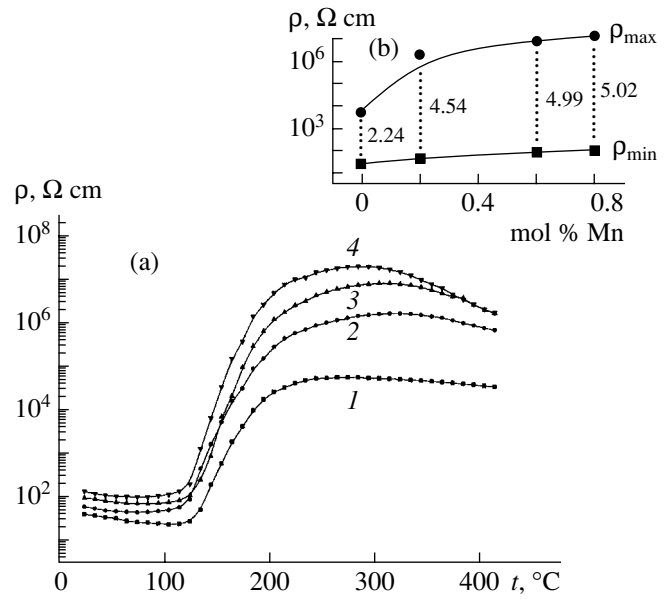


Fig. 1. (a) Temperature dependences of resistivity for $(\text{Ba}_{0.996}\text{Y}_{0.004})\text{TiO}_3$ PTCR ceramics containing (1) 0, (2) 0.2, (3) 0.6, and (4) 1 mol % Mn. (b) Composition dependences of ρ_{\max} , ρ_{\min} , and $\log(\rho_{\max}/\rho_{\min})$ (numbers between the curves).

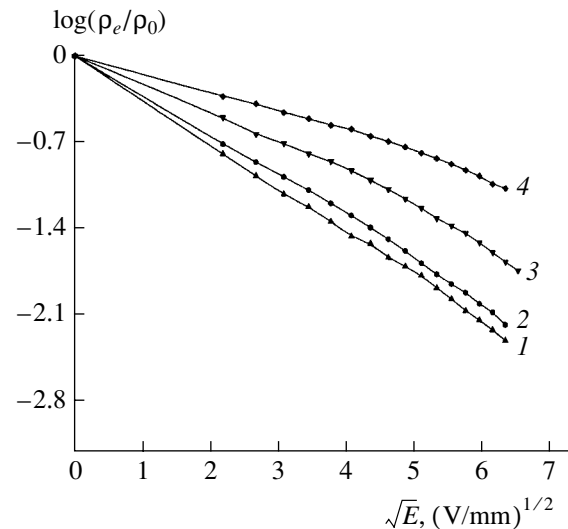


Fig. 2. Semilog plots of normalized resistivity vs. $E^{1/2}$ for $(\text{Ba}_{0.996}\text{Y}_{0.004})\text{TiO}_3$ PTCR ceramics containing (1) 0, (2) 0.2, (3) 0.6, and (4) 1 mol % Mn.

of Z''_{\max} and M''_{\max} are merely different representations of experimental data and are related by

$$M'' = \frac{\epsilon_0 Z''}{C R}. \quad (6)$$

Figure 4 shows the frequency dependences of room-temperature Z'' and M'' for $(\text{Ba}_{1-x}\text{Y}_x)\text{TiO}_3$ samples with

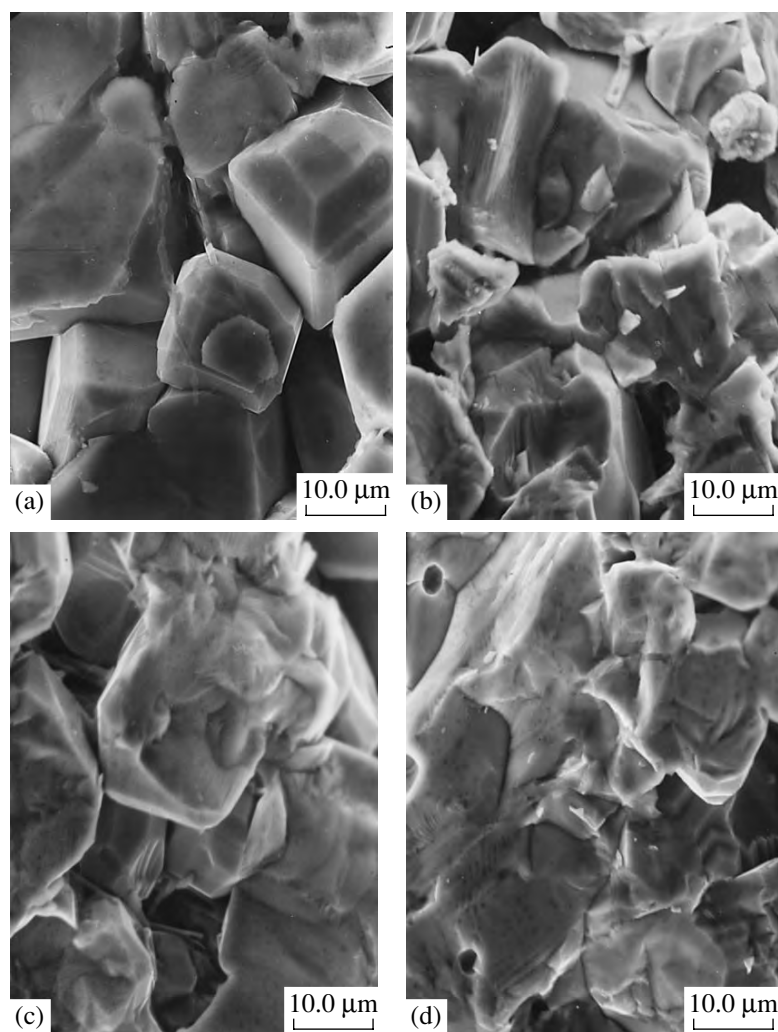


Fig. 3. Microstructures of $(\text{Ba}_{0.996}\text{Y}_{0.004})\text{TiO}_3$ PTCR ceramics containing (a) 0, (b) 0.2, (c) 0.6, and (d) 1 mol % Mn; $\times 2000$.

$x = 0.002, 0.003$, and 0.004 . The $Z''(f)$ curves show one peak ($\sim 10^4$ Hz at $x = 0.002$, $\sim 10^5$ Hz at $x = 0.003$, and $\sim 10^6$ Hz at $x = 0.004$), while the $M''(f)$ curves contain two peaks, one at intermediate frequencies ($\sim 10^5$ Hz at $x = 0.002$, $\sim 10^6$ Hz at $x = 0.003$, and $> 10^6$ Hz at $x = 0.004$) and the other at frequencies above 10^8 Hz.

A noteworthy feature of these data is that, independent of the yttrium concentration in $(\text{Ba}_{1-x}\text{Y}_x)\text{TiO}_3$, the peaks in Z'' and M'' differ in frequency. The likely reason is that these peaks originate from different regions of the ceramics [2–4]. In particular, the height and position of the peak in Z'' are governed by the electrical properties of grain boundaries, whereas the peak in M'' is influenced by the properties of the surface layer of the grains at intermediate frequencies and by those of the grain bulk at frequencies above 10^8 Hz.

Consequently, independent of the yttrium concentration in $(\text{Ba}_{1-x}\text{Y}_x)\text{TiO}_3$ PTCR ceramics, the grain bulk, surface layer, and grain boundaries differ in properties. By analyzing complex impedance and electric

modulus data obtained in a wide frequency range, one can evaluate the electrical properties of these regions. However, in the case of high-conductivity materials, the room-temperature electrical properties of the grain bulk and surface layer are difficult to distinguish because they differ little in resistance.

The temperature dependence of resistivity characteristic of PTCR ceramics (Fig. 5) consists of three distinct portions. In regions *I* and *III*, the temperature variation of resistivity is similar to that in semiconductors and dielectrics, respectively; in region *II*, resistance rises rapidly with temperature.

Figure 6 shows the frequency dependences of Z'' and M'' for $(\text{Ba}_{0.996}\text{Y}_{0.004})\text{TiO}_3$ ceramics in regions *I* (17 – 70°C), *II* (137 – 187°C), and *III* (237 – 287°C). In region *I*, Z'' decreases with increasing temperature, which is due, according to Eqs. (3) and (4), to a decrease in resistance. The shift of the peak in Z'' to higher frequencies is caused by a decrease in the capacitance of the RC circuit representing the grain bound-

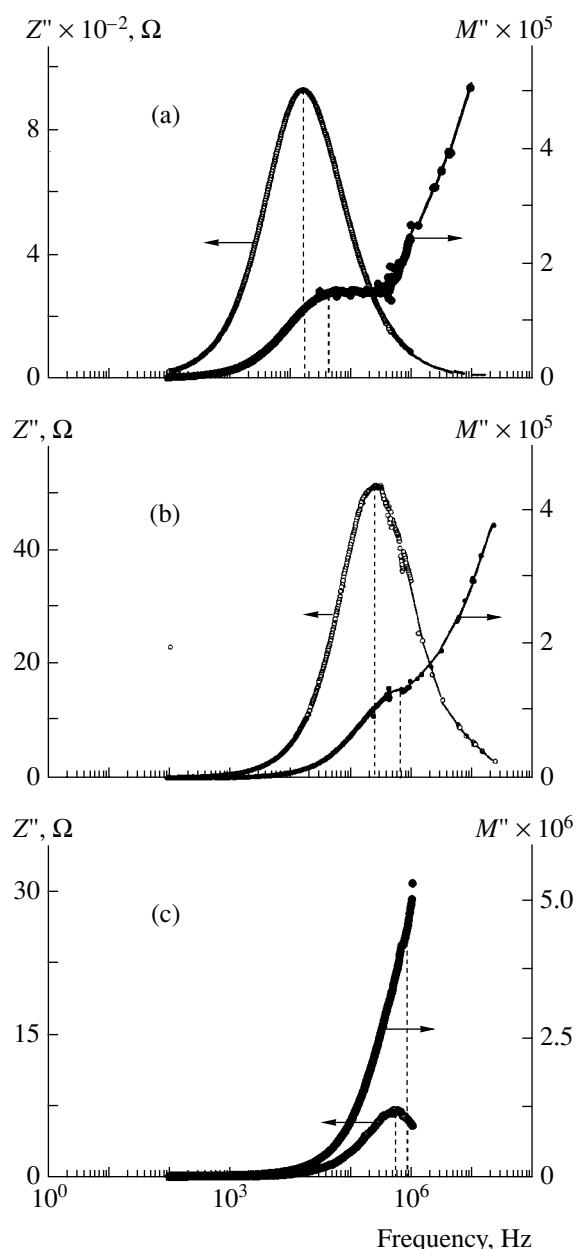


Fig. 4. Frequency dependences of Z' and M'' for (a) $(\text{Ba}_{0.998}\text{Y}_{0.002})\text{TiO}_3$, (b) $(\text{Ba}_{0.997}\text{Y}_{0.003})\text{TiO}_3$, and (c) $(\text{Ba}_{0.996}\text{Y}_{0.004})\text{TiO}_3$ PTCT ceramics at 20°C .

aries (Figs. 5, 6, region I). In region II, the peak in Z' shifts notably to lower frequencies with increasing temperature. Moreover, the peak becomes much stronger, which is due, according to Eqs. (3) and (4), to an increase in both the capacitance and resistance of the RC circuit (Figs. 5, 6, region II). In contrast to that in Z' , the peak in M'' shifts slightly to higher frequencies with increasing temperature, which is attributable, according to Eqs. (3) and (5), to a decrease in the resistance of the RC circuit representing the surface layer of the grains.

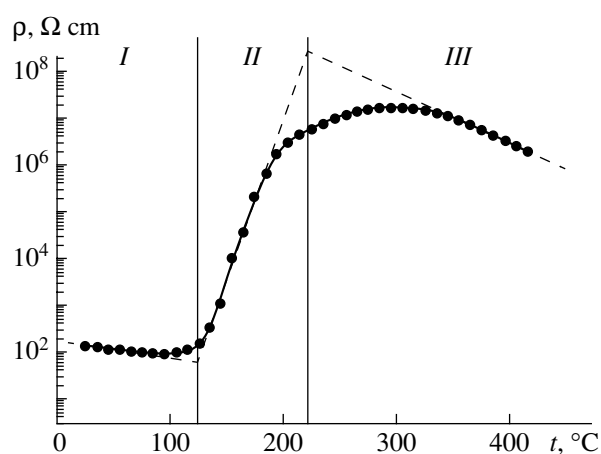


Fig. 5. Temperature dependence of resistivity characteristic of PTCT ceramics; (I–III) see text.

Using experimental data, we calculated the resistances of the grain bulk, surface layer, and grain boundaries in $(\text{Ba}_{0.996}\text{Y}_{0.004})\text{TiO}_3$ PTCT ceramics (Fig. 7). The grain bulk and surface layer are found to be close in resistance and its variation (monotonic) with temperature (curves 1, 2). Consequently, the PTCT behavior of Mn-free $(\text{Ba}_{0.996}\text{Y}_{0.004})\text{TiO}_3$ is due to changes in the electrical properties of the grain boundaries (curve 3).

The room-temperature resistance versus Mn content data for $(\text{Ba}_{0.996}\text{Y}_{0.004})\text{TiO}_3$ PTCT ceramics are presented in Fig. 8. With increasing Mn content, the grain-boundary resistance rises rapidly, whereas that of the grain bulk varies very little. The reason is that, in the concentration range studied, manganese does not penetrate into the grain bulk of PTCT barium titanate. In the Mn-doped samples, the room-temperature resistance of the surface layer was found to differ insignificantly from that of the grain bulk and could not be determined separately. At higher temperatures, the difference in resistance between the grain bulk and surface layer is more pronounced.

The temperature effect on the frequency dependences of Z' and M'' for Mn-doped materials (Fig. 9) differs from that for $(\text{Ba}_{0.996}\text{Y}_{0.004})\text{TiO}_3$ (Fig. 6): with increasing temperature, the peak in M'' shifts to lower frequencies, which is due, according to Eqs. (3) and (5), to an increase in the resistance of the RC circuit representing the surface layer of the grains. The resistances of the grain bulk, surface layer, and grain boundaries extracted from experimental data demonstrate that the surface layer and grain boundaries are similar in the temperature variation of resistance. The introduction of manganese into PTCT barium titanate also raises the grain-boundary resistance (Fig. 10).

To interpret the effect of Mn doping on the $\rho_{\text{max}}/\rho_{\text{min}}$ ratio in the PTCT region, we calculated the height of the intergranular barriers. In region I (Fig. 5), the tem-

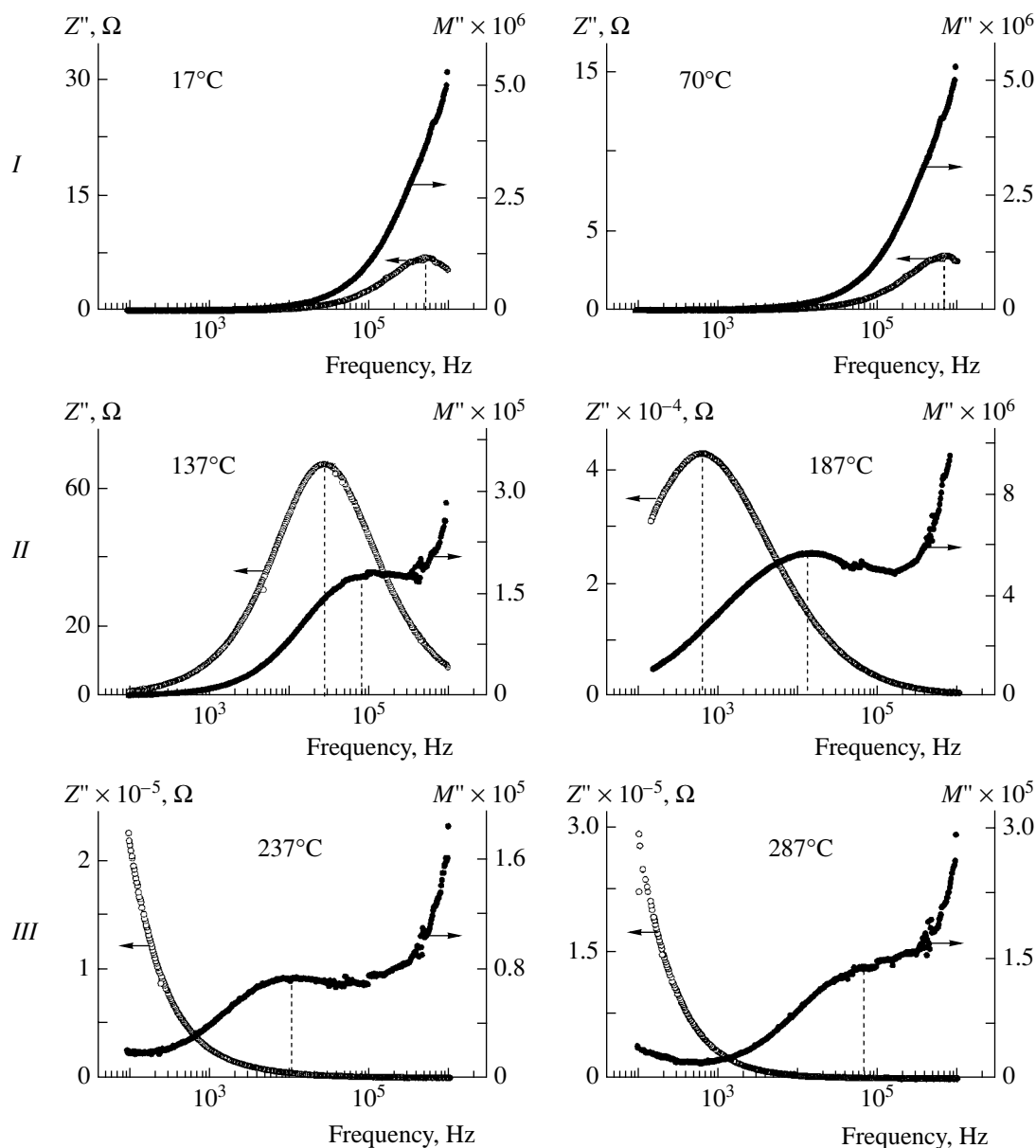


Fig. 6. Frequency dependences of Z'' and M'' for $(\text{Ba}_{0.996}\text{Y}_{0.004})\text{TiO}_3$ ceramics at different temperatures.

perature variation of resistance is described by the equation [1, 13]

$$\rho_s = \rho_0 e^{\frac{E_a^I}{kT}}, \quad (7)$$

where ρ_0 is a constant for barium titanate [14], E_a^I is the activation energy for conduction in region I, and k is the Boltzmann constant. A similar equation is applicable to region III [1, 13],

$$\rho_d = \rho_0^d e^{\frac{E_a^{III}}{kT}}, \quad (8)$$

where E_a^{III} is the activation energy for conduction in region III.

The temperature variation of resistance in region II (PTCR behavior) is commonly interpreted in the Heywang model [1],

$$\rho = \alpha \rho_s e^{\frac{\Phi_0(T)}{kT}}, \quad (9)$$

where α is a geometric factor, and $\Phi_0(T)$ is the intergranular barrier height:

$$\Phi_0(T) = \frac{e^2 n_D b^2}{2\epsilon_i(T)\epsilon_0}. \quad (10)$$

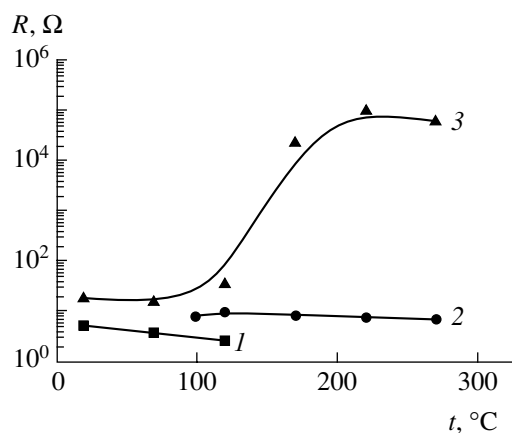


Fig. 7. Temperature dependences of resistance for the (1) grain bulk, (2) surface layer, and (3) grain boundaries in $(\text{Ba}_{0.996}\text{Y}_{0.004})\text{TiO}_3$ ceramics.

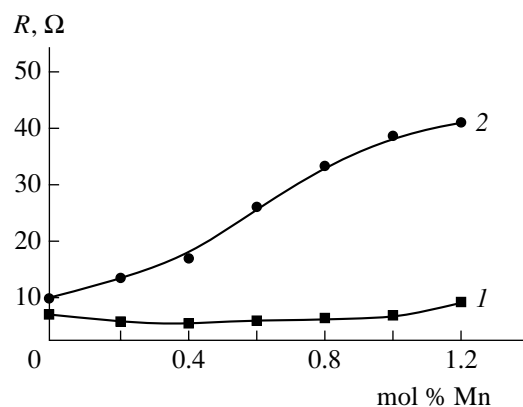


Fig. 8. Resistance as a function of Mn content for the (1) grain bulk and (2) grain boundaries in Mn-doped $(\text{Ba}_{0.996}\text{Y}_{0.004})\text{TiO}_3$ ceramics at 20°C .

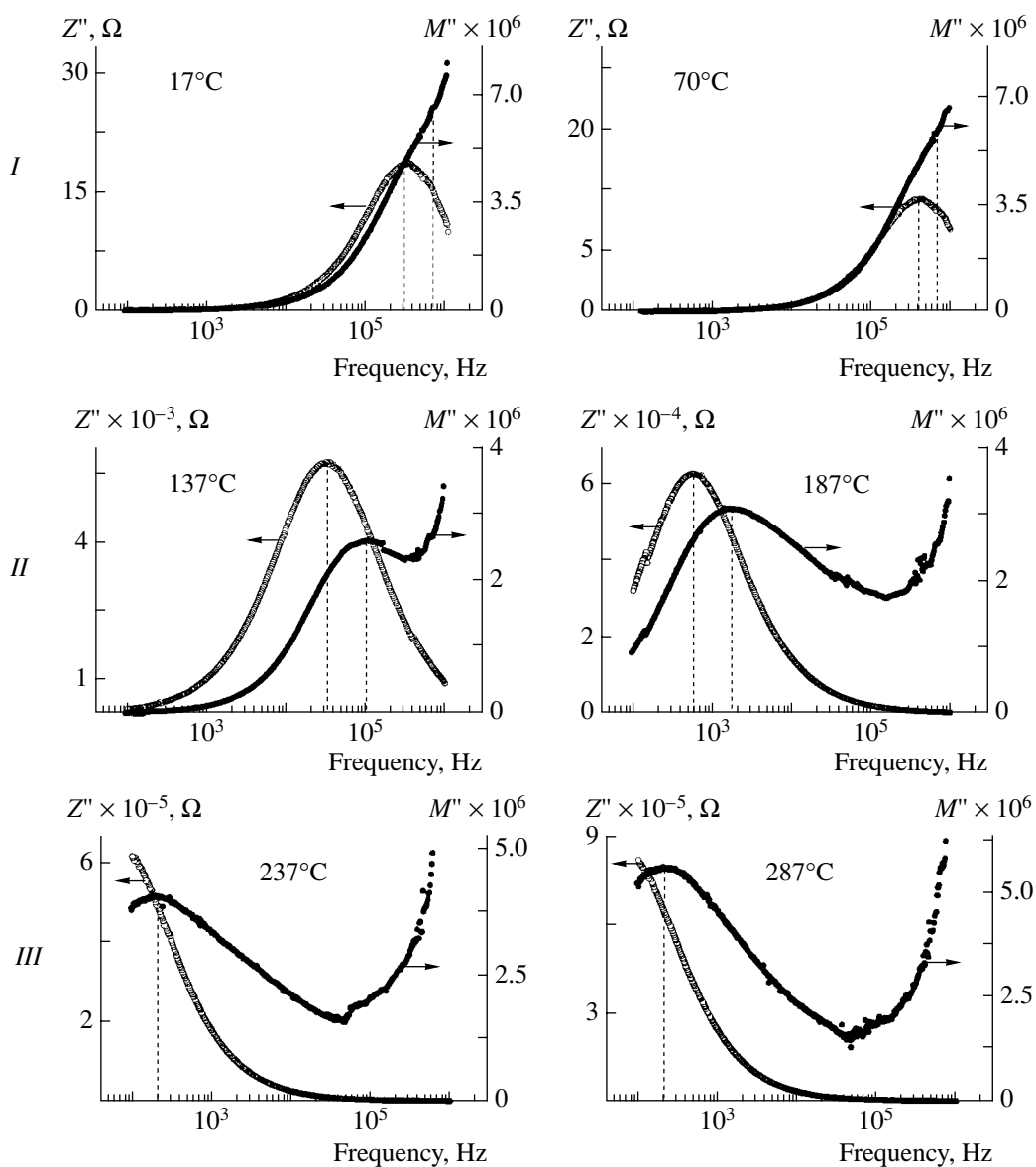


Fig. 9. Frequency dependences of Z'' and M'' for Mn-doped (0.6 mol %) $(\text{Ba}_{0.996}\text{Y}_{0.004})\text{TiO}_3$ ceramics at different temperatures.

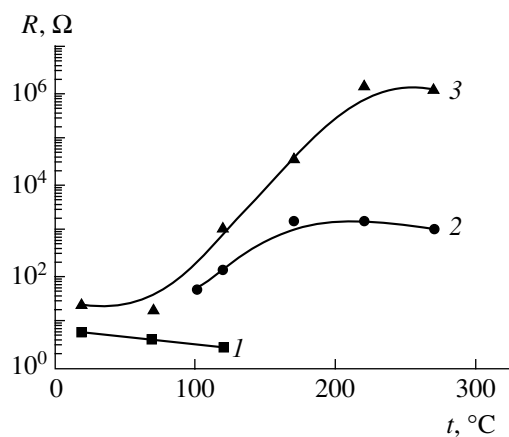


Fig. 10. Temperature dependences of resistance for the (1) grain bulk, (2) surface layer, and (3) grain boundaries in $(\text{Ba}_{0.996}\text{Y}_{0.004})\text{TiO}_3$ ceramics doped with 0.6 mol % Mn.

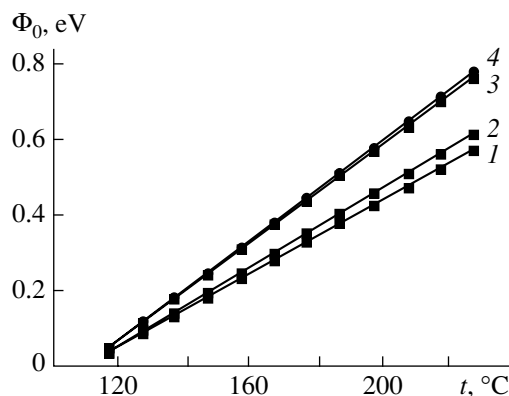


Fig. 11. Temperature dependences of the intergranular barrier height for $(\text{Ba}_{0.996}\text{Y}_{0.004})\text{TiO}_3$ ceramics containing (1) 0, (2) 0.6, (3) 0.8, and (4) 1.2 mol % Mn.

Here, e is the electronic charge (1.602×10^{-19} C), n_D is the bulk electron concentration, b is the barrier thickness ($2b = n_S/n_D$, where n_S is the surface concentration

of acceptor states), and $\epsilon_i(T)$ is the permittivity of the grain bulk. In ferroelectrics, ϵ_i follows the Curie–Weiss law, $\epsilon_i(T) = \frac{C}{T - \Theta}$, where C is the Curie constant and T_C is the Curie temperature (in barium titanate, $C = 1.7 \times 10^5$ K and $\Theta = 383$ K [13]).

From Eqs. (7) and (9), we obtain

$$\rho = \alpha \rho_0 e^{\frac{E_a^I}{kT}} e^{\frac{e^2 n_D b^2 (T - \Theta)}{2 \epsilon_0 C k T}}. \quad (11)$$

Calculations by Eqs. (7), (8), and (11) demonstrate that, in region I, ρ_0 increases with Mn content, while E_a^I decreases substantially. By contrast, in region III, ρ_0^d decreases, while the activation energy for conduction rises (table).

The results thus obtained were used to calculate, by Eq. (10), the intergranular barrier height Φ_0 as a function of Mn content in region II, where the resistance rises drastically (Fig. 11). It can be seen that, with increasing Mn content, the intergranular barrier grows, which accounts for the increase in the ρ_{\max}/ρ_{\min} ratio (Fig. 1). Our Φ_0 data for PTCR barium titanate agree with earlier results [15]. Thus, the introduction of the Mn acceptor into PTCR barium titanate leads to the formation of a high-resistance layer on the grain surface, thereby increasing the intergranular barrier height.

CONCLUSION

Our studies of Mn-doped $(\text{Ba}, \text{Y})\text{TiO}_3$ PTCR ceramics in broad temperature and frequency ranges demonstrate that the Mn content has a weak effect on the resistance of the grain bulk. The Mn ions, acting as acceptors, reside mainly at grain boundaries and in the surface layer of the grains. This markedly improves the properties of the PTCR materials, raising the ρ_{\max}/ρ_{\min} ratio and reducing the magnitude of the varistor effect.

REFERENCES

1. Heywang, W., Resistivity Anomaly in Doped Barium Titanate, *J. Am. Ceram. Soc.*, 1964, vol. 47, no. 10, pp. 484–490.
2. Sinclair, D.C., Morrison, F.D., and West, A.R., Applications of Combined Impedance and Electric Modulus Spectroscopy to Characterise Electroceramics, *Int. Ceram.*, 2000, vol. 2, pp. 33–37.
3. Morrison, F.D., Sinclair, D.C., and West, A.R., An Alternative Explanation for the Origin of the Resistivity Anomaly in La-Doped BaTiO_3 , *J. Am. Ceram. Soc.*, 2001, vol. 84, no. 2, pp. 474–476.
4. Morrison, F.D., Sinclair, D.C., and West, A.R., Characterization of Lanthanum-Doped Barium Titanate Ceramics Using Impedance Spectroscopy, *J. Am. Ceram. Soc.*, 2001, vol. 84, no. 3, pp. 531–538.

Effect of Mn content on properties of PTCR ceramics

Mole fraction of Mn	R_0, Ω	E_a^I, eV	$n_D b^2, \text{cm}^{-1}$	R_0^d, Ω	E_a^{III}, eV
0	1.5	0.09	9.1×10^8	1070	0.20
0.002	5.9	0.06	9.3×10^8	35.0	0.59
0.004	7.0	0.06	9.3×10^8	25.0	0.70
0.006	9.0	0.06	9.8×10^8	5.0	0.75
0.008	15.1	0.05	1.2×10^9	0.4	0.91
0.010	20.2	0.05	1.2×10^9	0.9	0.85
0.012	34.2	0.04	1.3×10^9	1.0	0.85

5. Yanchevskii, O.Z., V'yunov, O.I., Belous, A.G., and Vasil'ev, A.D., Effect of Mn-Containing Additions on the Properties of Semiconducting Barium Titanate, in *Elektronnaya mikroskopiya i prochnost' materialov* (Electron Microscopy and Strength of Materials), Kiev: Inst. Problem Materialovedeniya, 1997, pp. 106–113.
6. Kostikov, Yu.D. and Leikina, B.B., Effect of 3d Transition Metal Oxides on the PTCR Behavior of Ceramics Based on Semiconducting Barium Titanate, *Izv. Akad. Nauk SSSR, Neorg. Mater.*, 1990, vol. 26, no. 4, pp. 884–886.
7. Podkin, Yu.D. and Fedinchin, E.I., Extending the Frequency Range of Q-Meters, *Prib. Tekh. Eksp.*, 1977, no. 3, pp. 167–168.
8. Pavlov, A.N. and Raevskii, I.P., Varistor Effect in Semiconducting Ferroelectric Ceramics, *Zh. Tekh. Fiz.*, 1997, vol. 67, no. 12, pp. 21–25.
9. Gaosheng, L. and Roseman, R.D., Secondary Thermal Treatment Effect on PTCR BaTiO₃, *J. Mater. Sci. Lett.*, 1999, vol. 18, pp. 1875–1878.
10. Belous, A.G., Kolodyazhnyi, T.V., and Yanchevskii, O.Z., Varistor Effect in PTCR Ceramics Based on Semiconducting Barium Titanate, *Ukr. Khim. Zh.* (Ukr. Ed.), 1995, vol. 61, no. 8, pp. 86–89.
11. Jonker, G.H., Some Aspects of Semiconducting Barium Titanate, *Solid-State Electron.*, 1964, vol. 7, pp. 895–903.
12. Dutta, P.K. and Alim, M.A., The AC Electrical Behavior of Hydrothermally Synthesized Barium Titanate Ceramics, *Jpn. J. Appl. Phys.*, 1996, vol. 35, no. 12, pp. 6145–6152.
13. Heywang, W., Semiconducting Barium Titanate, *J. Mater. Sci.*, 1971, no. 6, pp. 1214–1226.
14. Wang, D.Y. and Umeya, K., Electrical Properties of PTCR Barium Titanate, *J. Am. Ceram. Soc.*, 1990, vol. 73, no. 3, pp. 669–677.
15. Hari, N., Padmini, P., and Kutty, T., Complex Impedance Analyses of *n*-BaTiO₃ Ceramics Showing Positive Temperature Coefficient of Resistance, *J. Mater. Sci.*, 1997, vol. 8, pp. 15–22.